Simultaneous small angle neutron scattering and Fourier transform infrared spectroscopic measurements on cocrystals of syndiotactic polystyrene with polyethylene glycol dimethyl ethers

Fumitoshi Kaneko,[a]* Naoki Seto,[a] Shuma Sato,[a] Aurel Radulescu,[b]* Maria Maddalena Schiavone,[b] Jürgen Allgaier,[c] and Koichi Ute[d]

[a] Graduate School of Science, Osaka University, Toyonaka, Osaka 560-0043, Japan.

[b]Forschungszentrum Jülich GmbH, Jülich Centre for Neutron Science, JCNS Aussenstelle am FRM II, Lichtenbergstraße 1, 85747, Garching, Germany.

[c]Jülich Centre for Neutron Science JCNS(JCNS-1) and Institute for Complex Systems (ICS), Forshungszentrum Jülich GmbH, 52425 Jülich, Germany,

[d]Department of Chemical Science and Technology, The University of Tokushima, Tokushima 770-8506, Japan

Correspondence e-mail: toshi@chem.sci.osaka-u.ac.jp, a.radulescu@fz-juelich.de

Syndiotactic polystyrene (sPS) is a crystalline polymer which has a unique property; it is able to form cocrystals with a wide range of chemical compounds, in which the guest molecules are confined in the vacancies of the host sPS crystalline region. Recently, it has been found that even polyethylene glycol oligomers with molecular weight more than several hundreds can be introduced into the sPS crystalline region. It is a quite important subject how such a long chain molecule is stored in the host sPS lattice. To tackle this issue, a new simultaneous measurement method of small angle neutron scattering and Fourier-transform infrared spectrum (SANS/FTIR), which we had developed recently, was applied to sPS cocrystal with polyethylene glycol dimethyl ether with molecular weight of 500 (PEGDME500). The temperature dependent changes of SANS profile and FTIR spectrum were followed from room temperature up to 140°C for a one-dimensionally oriented SANS/PEGDME500 cocrystal sample. The intensity of the reflections due to the stacking of crystalline lamellae showed significant temperature dependence. The 2D pattern in the high Q region of SANS also changed depending on temperature. The combined information obtained by SANS and FTIR suggested that PEGDME500 molecules are distributed in both the crystalline and amorphous regions in the low temperature region close to room temperature but they are dominantly included in the amorphous region in the high temperature region. It was also suggested by the 2D SANS profile that PEGDME500 molecules in the crystalline region have an elongated structure along the thickness direction of the crystalline lamellae.

Synopsis

A new simultaneous measurement method of small angle neutron scattering and Fourier-transform infrared spectrum was applied to a study on sPS cocrystal with polyethylene glycol dimethyl ether with molecular weight of 500. It was suggested that the guest molecules in the crystalline region have an elongated structure along the thickness direction of the crystalline lamellae.

1. Introduction

Syndiotactic polystyrene (sPS) is a crystalline polymer that possesses some intriguing properties. It crystallizes into several crystalline states with different conformation and lateral packing, depending on crystallization conditions and following treatments (Sorrentino & Vittoria, 2009). In addition to polymorphism, sPS forms cocrystals, where a variety of chemical compounds are included as guests into regularly arranged vacancies formed by host sPS chains of trans, trans, gauche, gauche (TTGG) conformation (Guerra *et al.*, 2009, 2012). The sPS cocrystals can be classified into four different kinds of groups, according to the crystal system and the shape of the spaces the guest molecules occupy: monoclinic δ clathrate (Chatani *et al.*, 1993, Tarallo, Schiavone & Petraccone, 2010), monoclinic δ intercalate (Tarallo *et al.*, 2006, Petraccone *et al.*, 2005), triclinic δ clathrate (Tarallo, Petraccone, *et al.*, 2010) and orthorhombic ε clathrate (Tarallo, Schiavone, Petraccone, *et al.*, 2010). So far, many different kinds of chemical compounds have already been incorporated into sPS cocrystals, such as dye (Uda, Kaneko, Tanigaki, *et al.*, 2005), fluorescent (Itagaki *et al.*, 2008, Del Mauro *et al.*, 2007), photo-reactive (Stegmaier *et al.*, 2005, D'aniello *et al.*, 2007), paramagnetic molecules (Albunia *et al.*, 2009, Kaneko *et al.*, 2006), and so on. There is a possibility that polymer crystalline region based functional materials can be developed by combining the properties of guest molecules and host sPS lattice (Pilla *et al.*, 2009).

It has been found that there is a strong affinity between the cavities of sPS host lattice and the chemical compounds consisting of ethylene oxide groups, $(-C_2H_4O-)_n$. The incorporation of this kind of chemical compounds was first found for cyclic crown ethers (Kaneko *et al.*, 2010, 2011), which was subsequently confirmed also in linear polyethylene glycols (PEGs) (Kaneko & Sasaki, 2011). Up to now, even PEGs with molecular weight more than 1000 have been confirmed to be able to become a guest in sPS cocrystals (Kaneko *et al.*, 2014). It is a very interesting issue how such long-chain compounds can be introduced into the crystalline cavities in the sPS lattice and which conformation they adopt. It might be desirable to utilize the information of both overall molecular shape and local molecular structure of PEGs for approaching this issue. For this purpose, we have tried to apply a new measuring method, a simultaneous measuring technique of small angle neutron scattering (SANS) and Fourier-transform infrared spectrum (FTIR) which we

developed recently (Kaneko *et al.*, 2015), to the cocrystal system of sPS with PEGs.

Small angle neutron scattering (SANS) has been employed in research that aims at analyzing the mesoscopic scale structures. In combination with partial deuteration technique, SANS is able to characterize the structure of a specific part in a complex system, which makes it unsubstitutable with any other method for structural analysis. SANS has established its unique position as a powerful tool for structural investigation of soft-matter and biological systems. Furthermore, SANS has extended its presence also in the research of time-dependent structure evolution. The scattering pattern of SANS is determined by the scattering length density (SLD) profile in the object under study. Therefore, it is of great difficulty to derive the sole solution for the arrangement of constituent components only from the scattering pattern of SANS, in particular, when the system of interest is a multicomponent system. If we get any other structural information from the same system, it would reduce greatly the difficulty of analyzing the SANS data. For this purpose, we tried to build an experimental system, which enables to measure the FTIR spectrum and SANS 2D profile from the same sample at the same time. FTIR spectroscopy has been employed as a complementary tool of X-ray and neutron diffractometry and provides information about the concentration and conformational state of each chemical species in a measuring object. Simultaneous analyses by X-ray scattering and Fourier transform infrared (FTIR) spectroscopy have been already developed for synchrotron radiation facilities (Nayer *et al.*, 1995, Innocenzi, *et al.*, 2005, Ratri & Tashiro, 2013). Similarly, the introduction of FTIR spectroscopy to SANS would produce a fruitful methodology for such a simultaneous measurement system. In a previous study (Kaneko *et al.*, 2015), we tested the simultaneous experimental setup to a sPS cocrystal system and confirmed its usefulness; the information obtained from the FTIR spectrum helped us greatly interpret the SANS profile changes.

In this study, we have investigated how the long chain of PEGs is stored in the crystalline region of sPS cocrystal by carrying out simultaneous SANS/FTIR measurements. For this purpose, we used the two strategies. One is the employment of the combination of fully deuterated host sPS and protonated guest PEG molecules, which highlights the guest PEG molecule in the host polymer matrix and provides the information about the distribution of PEG molecules between the crystalline and amorphous regions. Second is the temperature dependent measurement. The guest molecules in the sPS cocrystal tend to migrate into the amorphous region at elevated temperatures. Accordingly, the comparison of SANS and FTIR data between the lower and higher temperature regions would inform us the structural features of PEG in the crystalline and amorphous regions. In the previous simultaneous SANS/FTIR study using a short polyethylene glycol dimethyl ether (PEGDME), triethyleneglycol dimethyl ether (TEGDME) with molecular weight of 178, the guest molecules hardly remained in the amorphous region at elevated

temperatures because of the high volatility (Kaneko *et al.*, 2015). In response to this point, we employed a longer PEGDME with molecular weight of about 500 (PEGDME500). In this paper, it is shown at first that the SANS profile of sPS/PEGDME500 cocrystals changes significantly depending on temperature. Based on the SANS and FTIR results, it is demonstrated that PEG chains take a characteristic molecular shape and orientation in the crystalline region, which is far different from those residing in the amorphous region.

2. Experimental Section

2. 1. Samples

Fully deuterated syndiotactic polystyrene (d-sPS) (weight average molecular weight ($\overline{M}_w$) =1.1×10^5 and dispersity $Đ_M$ = 1.9) was synthesized according to the coordination polymerization developed by Ishihara (Ishihara *et al.*, 1986), using fully deuterated styrene with purity more than 98% purchased from Cambridge Isotope Lab. PEGDME500 was purchased from Sigma-Aldrich and used without further purification. Chloroform, acetone and their full deuterides (all purities were more than 98%) were purchased from Sigma-Aldrich and Armor Chemicals and used without further purification. Uniaxially oriented amorphous d-sPS samples about 50 μm thick were prepared by the following procedure; amorphous film samples of d-sPS were obtained by quenching a melt of sPS in an ice-water bath, drawing the melt-quenched d-sPS film four times in an oil bath kept at 373 K, and clipping well-oriented portions from the drawn film. The oriented amorphous films were exposed to a vapor of chloroform to give oriented samples of sPS/chloroform cocrystal. The cocrystal films were soaked into an PEGDME500/acetone mixture at about 1:1 in weight ratio for a few days to substitute the guest molecules and then kept in a vacuum oven at 40˚C for an hour to remove solvent acetone, giving uniaxially oriented sPS/PEGDME500 cocrystal films.

2. 2. Simultaneous SANS/FTIR measurement system

For simultaneous SANS/FTIR measurements, a device described in the previous report was used. The device consisting of a compact portable FTIR spectrometer (PerkinElmer, Spectrum Two) and an optical system of our own making was designed to be installed in the sample chamber of a SANS instrument. The concept of the simultaneous system is depicted in Fig. 1. The optical system consists of six mirrors (optical elements 1 to 6). Elements 3 and 4 (aluminum deposited quartz), which are irradiated by both the neutron beam (green line) and infrared beam (yellow line), work as a beam mixer and selector, respectively. They transmit the neutron beam efficiently but act as mirrors to reflect the infrared beam. The other four elements work as mirrors only for the infrared beam. The windows (elements 7 and 8) of the sample cell with a brass body wound with a copper tube to temperature control are KBr plates 2 mm thick. The two beams in the

system are made to run on the same line by element 3 and pass through the same sample position coaxially, and then they are separated from each other with element 4, entering into its own detector system.

Measurements All the simultaneous SANS/FTIR measurements were carried out by using the KWS2 diffractometer of the Jülich Centre for Neutron Science (JCNS), outstation at Heinz Maier-Leibnitz Center (MLZ) in Garching, Germany (Radulescu *et al.*, 2012). Scattering data were obtained using a two dimensional (2D) detector with active area of 60×60 cm^2 and 128×128 channels. A wavelength λ= 0.5 nm ($\Delta\lambda/\lambda$ = 20%) and a sample-to-detector distance of 4 m and 1.35 m were chosen. The typical measured sample area was about 5×5 mm^2. The one-dimensional intensity function $I_e(Q)$ along the equator was obtained from the corrected 2D data for detector sensitivity, instrumental noise, and scattering from empty cell, by reading pixel values and merging them with a proper width. The data accumulation time for each data point was 15 min. The temperature of the sample cell was controlled within the accuracy of ±0.5 K by circulating thermostated oil. The sample was kept under a slow flow of air. Transmission IR spectra were taken at a resolution of 2 cm^{-1} and a 10 min interval. The average accumulation time and the number of scans were 10 min and 128, respectively. For measuring time dependence of IR spectra and analyzing them, a commercially available software (PerkinElmer, Timebase) was employed. Wide angle X-ray scattering (WAXS) measurements were carried out by using CuKα radiation and an imaging plate of Fuji film Co.

3. Results and Discussion

3.1. Temperature Dependent Change of SANS Profile and FTIR Spectrum

The temperature dependence of 2D SANS profile is shown in Fig. 2. The two reflections due to the crystalline lamellae with repeat period of about 100Å appear along the meridian. The intensity of the lamellar reflection increases remarkably with temperature, which is a dramatic contrast with sPS/TEGDME cocrystal whose lamellar reflections wane as the temperature increases (Kaneko *et al.*, 2015). It follows that there is an evident difference in the temperature dependence of guest distribution between the d-sPS/TEGDME and d-sPS/PEGDME500 cocrystals, since the distribution of protonated guest molecules is the main factor to determine the scattering length density (SLD) in the host d-sPS matrix. The FTIR spectra measured in parallel with SANS 2D images (Fig. 3) also suggest that the PEGDME500 component behaves in a completely different manner from the TEGDME component. As for d-sPS/TEGDME cocrystal, the bands ascribed to C_2H_4O repeat unit, such as C-H stretch around 2874 cm^{-1}, decrease in intensity as the temperature increases and almost disappear around 140 ºC, whereas such drastic intensity changes do not take place in d-sPS/PEGDME500 cocrystal except for a slight intensity decrease at the temperatures

above 100 ºC. With respect to the bands due to host d-sPS, such as C-D stretch in the region of 2300 to 2150 cm^{-1}, both d-sPS/TEGDME and d-sPS/PEGDME500 cocrystals do not show any significant intensity changes during the course of temperature change. The difference in IR spectral changes is attributable to the volatility. The short TEGDME molecule is so volatile that it dissipates from the film as the temperature increases. On the other hand, PEGDME500 can be considered to remain in the film even at high temperatures. The slight intensity decrease of the C-H stretch band in the elevated temperature range is due to the partial degradation of PEGDME500. As shown in Fig. 3, a band around 1728 cm^{-1} appears and clearly increases in intensity with temperature. The 1728 cm^{-1} band can be assigned to the carbonyl stretch mode ν(C=O) due to the aldehyde group of low-mass products by the thermal decomposition of polyethylene glycol, which starts even in relatively moderate conditions (Bortel *et al.*, 1979, Han *et al.*, 1996). Such low mass products would gradually dissipate into the outside. Therefore, it can be inferred that a small amount of PEGDME500 is lost from the film owing the thermal decomposition at elevated temperatures, which results in the slight intensity decrease of the C-H stretch band.

According to the previous studies on sPS/PEGDME cocrystals (Kaneko & Sasaki, 2011), an appreciable amount of PEGDME500 is included also in the amorphous region, which would reduce the SLD contrast between the crystalline and amorphous regions. Actually, the lamellar reflections is narrowly observable at 25 ºC, as shown in Fig. 2. The guest molecule in the sPS cocrystal tends to migrate into the amorphous region as the temperature increases; although stabilized enthalpically by the host lattice at lower temperatures, the guest molecule in the amorphous region gains a larger entropic benefit such as higher conformational degree of freedom in the amorphous region at higher temperatures. In addition, the sPS cocrystal transforms to the γ phase around 130 ºC, in which the cavities between the TTGG helices of host sPS lattice shrink, pushing the guest molecules into the amorphous region. Taking into the account these properties of sPS cocrystal and also the FTIR results, the significant intensity increase of the lamellar reflection seen in SANS can be ascribed to the migration of PEGDME500 molecules into the amorphous region; the protonated PEGDME500 molecules are accumulating in the amorphous region as the temperature rises, and as a result, the SLD contrast between the crystalline and amorphous regions increases, as schematically illustrated in Fig. 4. The lamellar reflection shifts towards low *Q* at the elevated temperature (Fig. 5), which is ascribable to the expansion of the amorphous region caused by the guest transfer from the crystalline region to the amorphous region.

3. 2. Anisotropic SANS Profile at High Q Region

The 2D SANS profile in high Q region also shows significant difference between low and high temperatures, as shown in Fig. 6. The d-sPS/PEGDME cocrystal exhibits a clearly anisotropic scattering profile at 25 ºC. The scattering intensity slowly decreases along the equator and rapidly along the meridian. The anisotropy gradually ceases as the temperature increases and the scattering profile becomes almost isotropic at 140 ºC; the scattering tail along the equator is not observed. As shown in Fig. 6(c) and (d), such anisotropic characters do not appear in both the high and low Q regions before the guest exchange procedure. It follows that the SANS 2D profile reflects the molecular shape of guest PEGDME500 in the sPS film. Based on the temperature dependence of 2D profile, it can be inferred that PEGDME500 takes an elongated structure along the normal of the crystalline lamellae when it resides in the crystalline region, whereas it forms an isotropic structure after migrating into the amorphous region.

3. 3. Overall Pictures of PEGDME500 in Crystalline and Amorphous Regions

Contrary to the SANS profile along the meridian where the lamellar reflections emerge, there is no appreciable contribution of the lamellar stacking structure to the SANS profile along the equator. Accordingly, the molecular shape of the guest PEGDME500 is the principal factor to determine the equatorial profile. Fig. 7 shows the comparison of one-dimensional intensity function $I_e(Q)$ along the equator between two measuring temperature, 25 and 140ºC, together with the data of the sample before guest exchange treatment. As can be seen from this comparison, for the guest PEGDME500 there are significant differences in the Q dependence between 25 and 140ºC. In the double logarithmic plot, $I_e(Q)$ decays with a slope of -1 at 25ºC and -4 at 140ºC, suggesting that PEGDME500 takes a form of rod and sphere, respectively. The fitting of the $I_e(Q)$ data at 25ºC using a cylindrical model (Pedersen, 1997) provides a rod with a length of 40Å and a radius of 3Å. As for the $I_e(Q)$ data at 140ºC, its Kratky plot (Fig. 8) is characterized by a maximum around Q=0.06Å^{-1} and a gradual increase starting around Q=0.15Å^{-1}; the former suggests an existence of a compact body and the latter suggests structural looseness. Taking into account the structural features obtained from Figs 7 and 8, we adopt a star polymer like structure for PEGDME100 in the amorphous region, i.e., an agglomerate of PEGDME500 molecules where PEG chain branches emanating from a central dense core. The radius of gyration R_g of 33Å and the Flory exponent ν of 0.65 are derived by the fitting of the $I_e(Q)$ data at 140ºC using the following equation given by Dozier al. (1991),

$$I(Q) \propto I_0 \exp\left[-\frac{1}{3}Q^2 R_g^2\right] + \frac{4\pi\alpha}{Q\xi}\frac{\sin\left[\mu \tan^{-1}(Q\xi)\right]}{\left[1+Q^2\xi^2\right]^{\mu/2}}\Gamma(\mu),$$

where ξ is the correlation length inside the star, μ is a parameter related to ν as $\mu=1/\nu-1$, $\Gamma(\mu)$ is the gamma function with argument μ, and α is a parameter to be determined. The value of the obtained Flory exponent ν is larger than 1/2 for a random-walk chain and 3/5 for a self-avoiding random-walk chain, suggesting a rather stretched form of the PEG branches.

3. 4. Arrangements of PEGDME500 Chains in Crystalline Regions of sPS Cocrystal

The SANS results described in the previous section strongly suggest that the PEGDME500 molecules included in the crystalline region tend to takes an elongated structure in the direction perpendicular to the crystalline lamellar plane. The infrared spectrum measured in parallel with SANS shows some consistent spectral features of PEG chains. For example, the bands at 950, 1250 and 1300 cm^{-1} appear more distinctly at 25 ºC than at elevated temperatures, as shown in Fig. 9, which indicates that the guest PEGDME500 molecules form a more elongated structure with higher content of trans conformation when incorporated into the crystalline region (Deng *et al.*, 2006). PEG takes a regular helical conformation in the crystalline state, which can be regarded approximately as a uniform (7/2) helix, consisting of the regular repetition of *trans-trans-gauche* (TTG) type conformation (Takahashi *et al.*, 1973). It has been also confirmed that such a regular helix conformation gradually forms when a PEG solution is cooled (Kobayashi & Kitagawa, 1997). When taking a long helical structure, PEG chains exhibit some sharp conformational regularity bands assigned to the A_2 and E_1 modes of regular chain, such as 1345 cm^{-1} A_2 band (Yoshihara *et al.*, 1964, Matsuura & Miyazawa, 1969). The sPS/PEGDME500 cocrystal does not show such sharp conformational regularity bands. Taking these IR spectral features into account, it can be inferred that although the PEGME500 molecules do not form a uniform regular helical structure, they take elongated molecular forms as a whole along the thickness direction in the crystalline lamellae.

The elongated molecular shape seems to be consistent with the following structure features of sPS cocrystals. First, the length about 40Å obtained by SANS analysis is comparable to the crystalline lamellar thickness (Kaneko, Radulescu *et al.*, 2013). Second, on the guest exchange process, the new guest PEGDME500 might enter into the crystalline lamellae from the wide lamellar surface and proceed to the interior. If this happens, the new guest molecules would be apt to align perpendicular to the lamellar surface.

According to the previous work on sPS cocrystals with PEGDMEs (Kaneko & Sasaki, 2011, Kaneko *et al.*, 2014), the δ monoclinic clathrate having isolated cavities is generated by the guest exchange treatment on cast-grown sPS cocrystal samples. When carrying out the guest exchange procedure on one-dimensionally stretched sPS cocrystal sample, two kinds of cocrystal structures, major component monoclinic δ cocrystal and minor component orthorhombic ε cocrystal having

long-tube like hollows, are generated (Kaneko, Seto *et al.*, 2013). Actually, the coexistence of the δ and ε cocrystals is confirmed by the WAXS data of the d-sPS sample used for the simultaneous SANS/FTIR measurements, as shown in Fig. 10. The sample exhibits primarily the intense reflections of the γ phase, to which the δ and ε cocrystals have transformed on the heating process to 413K, but also the weak reflections due to the δ and ε cocrystal components remaining in the sample. It is also suggested by the 2D SANS profile that PEGDME500 molecules in the crystalline region have an elongated structure along the thickness direction of the crystalline lamellae. The hollow tube of the orthorhombic ε cocrystal is suitable to accommodate the elongated shaped PEGDME500 molecules, and besides the contribution of the monoclinc δ cocrystal seems to be important. As described in the previous section, the d-sPS/PEGDME500 cocrystal sample exhibits a clear anisotropic SANS profile, which suggests that the PEGDME molecule is highly oriented not only in the minor ε-type cocrystal region but also in the major δ-type cocrystal region.

The following points would assist the possibility of the elongated PEGDME molecules in the δ cocrystal region. First, it has been confirmed that the guest molecules in the monoclinic δ cocrystal region are quite replaceable (Uda *et al.*,2004, Yoshioka & Tashiro, 2003, Kaneko & Tsuchida, 2013). The chain molecules, such as n-alkanes, and aromatic molecules like toluene and xylene, can be substituted easily, without destruction of sPS structure. It can be inferred that the lattice of sPS cocrystal allows such small compounds to pass through the lattice, beyond the barrier between the cavities. Second, it has been also shown that the cavities are interconnected with narrow channels and, therefore, small gas molecules (such as helium and neon) are able to pass through the cocrystal lattices (Tamai & Fukuda, 2003, 2004). Third, the potential barrier around C-C bond connecting the phenyl-side group and the main chain is low (Schaefer *et al.*, 1988), which means that the flat plane of the phenyl side group is adjustable according to the shape of the guest molecules. Forth, the oxygen atom in the C_2H_4O repeat unit has a smaller diameter than the methylene CH_2 group and the rotational potential around the C-O bond is shallower than that of the C-C bond (Anderson & Wison, 2005). With these points taken into account, it seems plausible that a flexible PEG chain occupies several cavities of the delta cocrystal at the same time, in other words, the PEGDME500 molecule would be able to straddle several cavities along the *c* axis of the sPS delta cocrystalline region.

Further more detailed studies are necessary to obtain the more detailed structure information about the packing mode of PEG chain in the sPS cocrystalline regions and to confirm the accommodation of elongated PEG molecules in both types of sPS cocrystal. We are now conducting a systematic study using a series of PEGDME molecules with a wide range of molecular weight.

4. Conclusion

The cocrystal structure of sPS with PEGDME500 has been studied by employing simultaneous SANS and FTIR measuring method and the combination of deuterated polymer matrix sPS and protonated guest PEGDME500. The temperature dependent measurements of 2D SANS profile and FTIR spectrum provided the structural information about PEGDME500. The PEGDME500 molecules stored in the crystalline region showed a clear 2D anisotropic scattering profile, which indicated an elongated form perpendicular to the lamellar plane. On the other hand, the PEGDME500 molecules residing in the amorphous region exhibited an isotropic scattering profile, which suggested an agglomerate of PEGDME500 molecules having a dense core and loose arms. The FTIR spectra measured in parallel with SANS also suggested a stretched form of PEGDME500 molecules in the cocrystalline region.

This research was partly supported by a Grant-in-Aid for Scientific Research (KAKENHI (C) # 09014728 and 25410014) from the Japan Society for the Promotion of Science (JSPS). As for the preparation of deuterated sPS samples, the authors are grateful to the following people for their kind cooperation: Mr K. Kaji of Tosoh Finechem Corporation, Mr T. Tamada of Graduate School of Engineering Scinece, Osaka University, Mr M. Masaoka, Ms T. Arai, Prof A. Hashidzume, Dr Y. Takashima, Dr T. Okamura of Graduate School of School of Science, Osaka University, Mr K. Nishimura of Toyobo Co. and Dr N. Tanigaki of AIST. The authors deeply appreciate Mr. M. Nishiyama of Renovation Center of Instruements for Science Education and Technology, Osaka University for his kind support during the preparation of the experimental setup. As for the WAXS measurements, the authors thank Dr O. Tallaro of University of Naples Federico II for his kind support.

340 **References**

341 Albunia, A. R., D'Aniello, C., Guerra, G., Gatteschi, D., Mannini, M. & Sorace, L. (2009). *Chem*
342 *Mater* **21**, 4750-4752.

343 Anderson, P. M. & Wilson, M. R. (2005) *Mol. Phys.* **103**, 89–97.

344 Bortel, E., Hodorowicz, S., & Lamot, R. (1979). *Makromol. Chem*. **180**, 2491–2498.

345 Chatani, Y., Shimane, Y., Inagaki, T., Ijitsu, T., Yukinari, T. & Shikuma, H. (1993). *Polymer* **34**,
346 1620-1624.

347 D'aniello, C., Musto, P., Venditto, V. & Guerra, G. (2007). *J Mater Chem* **17**, 531-535.

348 Del Mauro, A. D. G., Carotenuto, M., Venditto, V., Petraccone, V., Scoponi, M. & Guerra, G. (2007).
349 *Chem Mater* **19**, 6041-6046.

350 Deng, Y., Dixon, J. B. & White, J. N. (2006) *Colloid Polym Sci* **284**, 347-356.

351 Dozier, W. D., Huang, J. S. & Fetters, L. J. (1991) *Macromolecules* **24**, 2810-2814.

352 Guerra, G., Albunia, A. R. & D'Aniello, C. (2009). *Syndiotactic Polystyrene: Synthesis,*
353 *Characterization, Processing, and Applications,* edited by J. Schellenberg, pp. 194-237.
354 Hoboken: Wiley.

355 Guerra, G., Daniel, C., Rizzo, P. & Tarallo, O. (2012). *J Polym Sci Pol Phys* **50**, 305-322.

356 Han, S., Kim, S. & Kwon, D. (1997) *Polymer* **38**, 317-323.

357 Innocenzi, P., Malfatti, L., Kidchob, T., Costacurta, S., Falcaro, P., Piccinini, M., Marcelli, A.,
358 Morini, P., Sali, D., Amenitsch, H. (2007). *J. Phys. Chem. C* **111**, 5345-5350.

359 Ishihara, N., Seimiya, T., Kuramoto, M. & Uoi, M. (1986). *Macromolecules* **19**, 2464-2465.

360 Itagaki, H., Sago, T., Uematsu, M., Yoshioka, G., Correa, A., Venditto, V. & Guerra, G. (2008).
361 *Macromolecules* **41**, 9156-9164.

362 Kaneko, F., Kashihara, N., Tsuchida, T. & Okuyama, K. (2010). *Macromol. Rapid Commun.* **31**,
363 554–557.

364 Kaneko, F., Radulescu, A. & Ute, K. (2013). *Polymer* **54**, 3145-3149.

365 Kaneko, F. & Sasaki, K. (2011). *Macromol Rapid Comm* **32**, 988-993.

366 Kaneko, F., Sasaki, K., Kashihara, N. & Okuyama, K. (2011). *Soft Materials* **9**, 107-123.

367 Kaneko, F., Seto, N., Sasaki, K., Sakurai, S., Kimura, G. (2013). *Macromol. Chem. Phys.* **214**,
368 1893−1900.

369 Kaneko, F., Seto, N., Sasaki, K., & Sakurai, S. (2014). *Chem. Lett*. **43**, 904-906.

370 Kaneko, F., Seto, N., Sato, S., Radulescu, A., Schiavone, M. M., Allgaier, J., Ute, K. (2015) *Chem.*
371 *Lett*. **44**, 497-499.

372 Kaneko, F. & Tsuchida, T. (2013). *Polymer* **54**, 760-765.

373 Kaneko, F., Uda, Y., Kajiwara, A. & Tanigaki, N. (2006). *Macromol Rapid Comm* **27**, 1643-1647.

374 Kobayashi, M. & Kitagawa, K. (1997). *Macromol. Symp.* **114**, 291-296.

Matsuura, H. & Miyazawa T. (1969) *J. Polym. Sci. A-2*, **7**, 1735-1744.

Naylor, S., Bras, W., Derbyshire, G., Mant, G. R., Bogg, D., Ryan, A. J. (1995) *Nucl. Instrum. Methods Phys. Res., Sect. B Res.* **97**, 253-256.

Pedersen, J. S. (1997) *Adv. Colloid Interface Sci.* **70**, 171-210.

Petraccone, V., Tarallo, O., Venditto, V. & Guerra, G. (2005). *Macromolecules* **38**, 6965-6971.

Pilla, P., Cusano, A., Cutolo, A., Giordano, M., Mensitieri, G., Rizzo, P., Sanguigno, L., Venditto, V. & Guerra, G. (2009). *Sensors* **9**, 9816-9857.

Radulescu, A., Pipich, V. & Ioffe, A. (2012). *Nucl Instrum Meth A* **689**, 1-6.

Ratri, P. J. & Tashiro, K. (2013) *Polym. J.* **45**, 1019-1026.

Schaefer, T., Sebastian, R., Penner, G. H. (1988). *Can. J. Chem.* **66**, 1495-1499.

Sorrentino, A. & Vittoria, V. (2009). *Syndiotactic Polystyrene: Synthesis, Characterization, Processing, and Applications*, edited by J. Schellenberg, pp. 157-192. Hoboken: John Wiley & Sons, Inc.

Stegmaier, P., Del Mauro, A. D., Venditto, V. & Guerra, G. (2005). *Adv Mater* **17**, 1166-+.

Takahashi, Y. Sumita, I. & Tadokoro, H. (1973). *J. Polym. Sci. Polym. Phys.* (1973). **11**, 2113-2122.

Tamai, Y. & Fukuda, M. (2004). *J. Chem. Phys.* **121**, 12085-12093.

Tamai, Y. & Fukuda, M. (2003). *Polymer* **44**, 3279-3289.

Tarallo, O., Petraccone, V., Albunia, A. R., Daniel, C. & Guerra, G. (2010). *Macromolecules* **43**, 8549-8558.

Tarallo, O., Petraccone, V., Venditto, V. & Guerra, G. (2006). *Polymer* **47**, 2402-2410.

Tarallo, O., Schiavone, M. M. & Petraccone, V. (2010). *Eur Polym J* **46**, 456-464.

Tarallo, O., Schiavone, M. M., Petraccone, V., Daniel, C., Rizzo, P. & Guerra, G. (2010). *Macromolecules* **43**, 1455-1466.

Uda, Y., Kaneko, F. & Kawaguchi, T. (2004). *Polymer* **45**, 2221-2229.

Uda, Y., Kaneko, F., Tanigaki, N. & Kawaguchi, T. (2005). *Adv Mater* **17**, 1846-+.

Yoshihara,T., Tadokoro, H., Murahashi, S. (1964). *J. Chem. Phys.* **41**, 2902-2911.

Yoshioka, A. & Tashiro, K. (2003). *Macromolecules* **36**, 3593-3600.

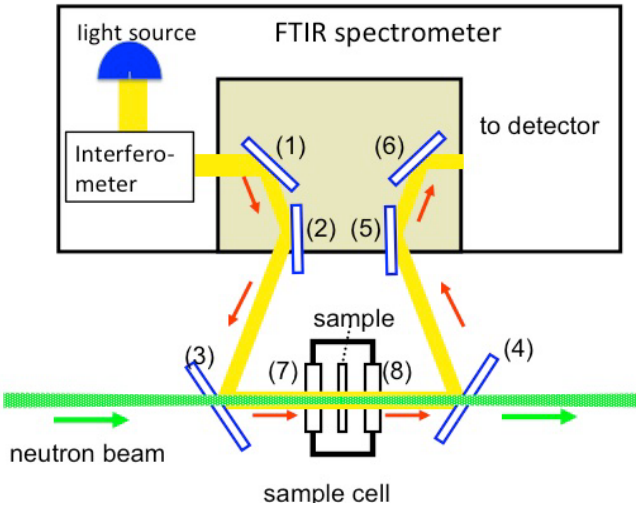

Fig. 1. Schematic drawing of the optical system for simultaneous measuring system of small angle neutron scattering with Fourier transform infrared spectroscopy. Parts 1 to 6 are mirrors and parts 7 and 8 are windows of the sample cell. The infrared and neutron beams are represented with yellow and green lines.

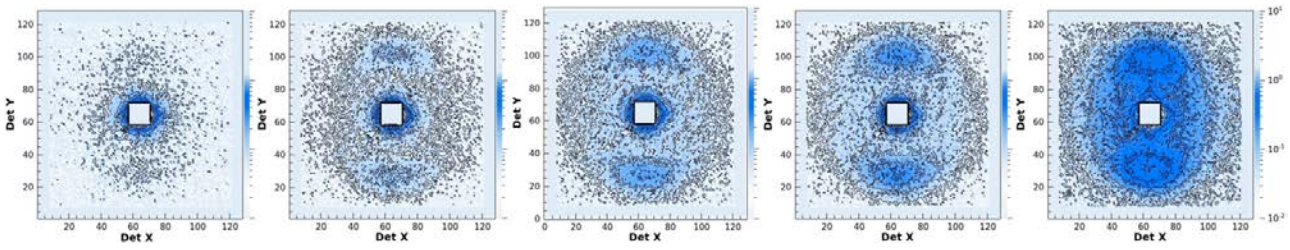

298 K 333 K 353 K 373 K 413 K

Fig. 2. Temperature dependence of small angle neutron scattering 2D images (with camera length of 4 m).

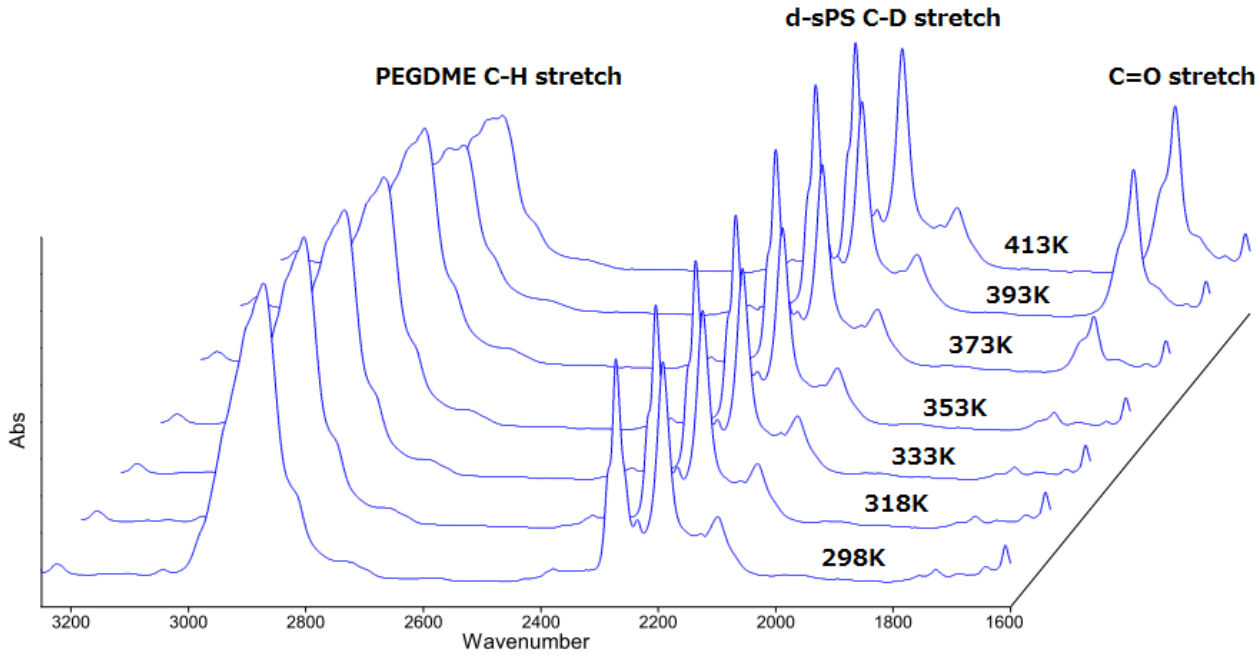

Fig. 3. Infrared spectral changes measured in parallel with small angle neutron scattering measurements

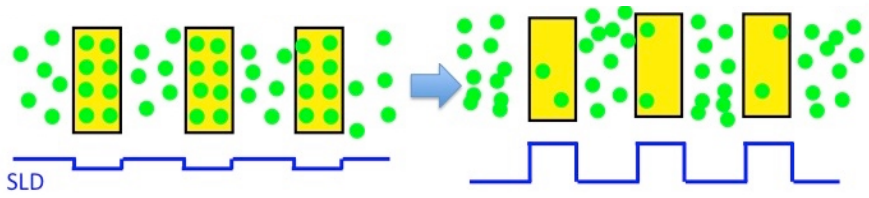

low temperature high temperature

Fig. 4. Schematic representation for temperature dependent distribution change of guest molecules. The solid state of d-syndiotactic polystyrene cocrystal containing polyethylene glycol dimethyl ether (PEGDME) with molecular weight of 500 is depicted as a one-dimensional array of crystalline lamellae (yellow box) and interlamellar amorphous regions. The green circles represent guest PEGDME molecules. The blue rectangle wave below represents the variation of scattering length density (SLD) between the crystalline and amorphous regions.

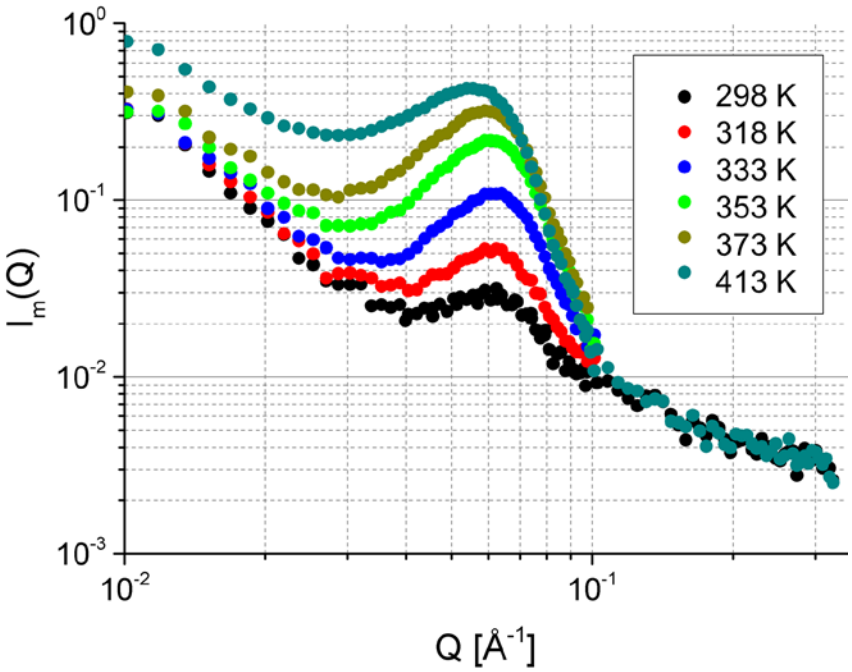

Fig. 5. Temperature dependence of SANS one-dimensional intensity functions, $I_m(Q)$, along the meridian.

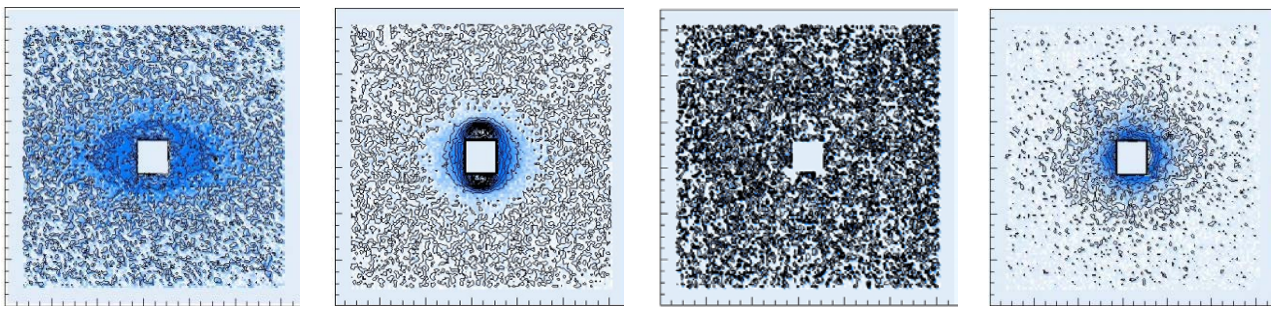

(a) (b) (c) (d)

Fig. 6. SANS 2D Profiles measured with a shorter camera length of 1 m (a-c) and 4m (d). (a) and (b): d-sPS/PEGDME500 at 298 and 413 K, (c) and (d) d-sPS film at 298 K before guest exchange treatment.

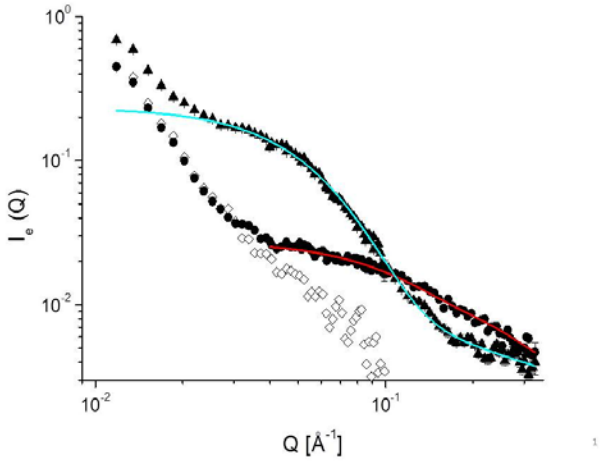

Fig. 7. One-dimensional intensity function of d-sPS/PEGDME500 along the equator, $I_e(Q)$, measured at 298 and 413 K (solid circles and triangles) and of the sPS/$CDCl_3$ before guest exchange (open diamonds).

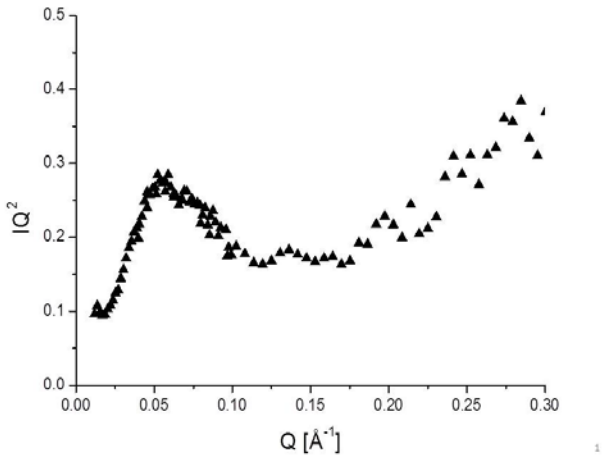

Fig. 8. Kratky plot obtained from $I_e(Q)$ data at 413K .

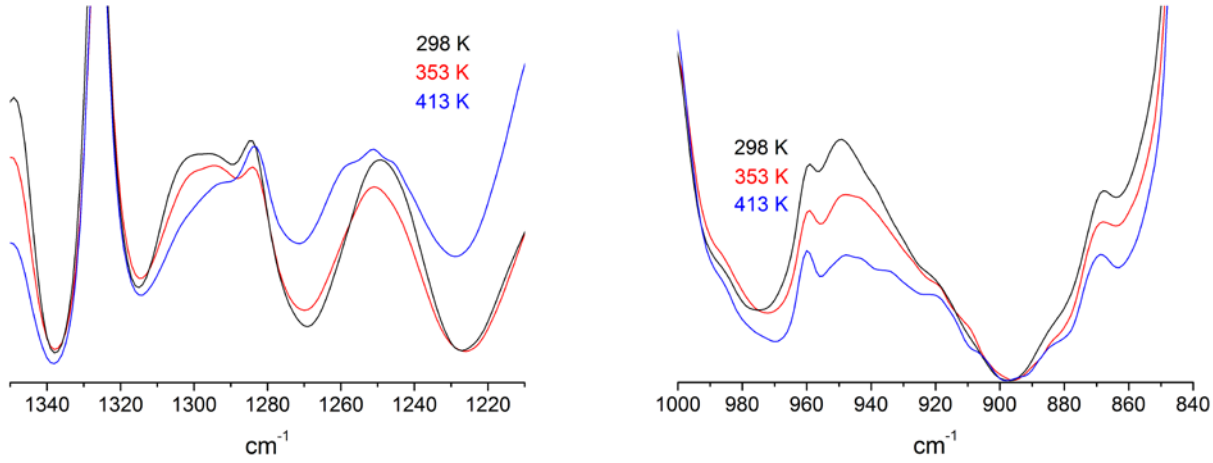

Fig. 9. Infrared spectral changes on heating process in sPS/PEGDME500, measured in parallel with SANS.

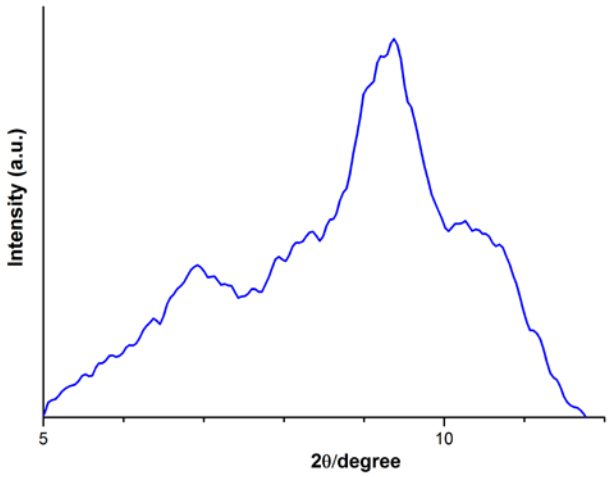

Fig. 10. WAXS profile measured along the equatorial direction of the d-sPS cocrystal specimen after the simultaneous SANS/FTIR measurements on heating process from 298 K to 413 K. The reflections characteristic of the γ phase appear at 9.4 and 10.5°. The reflections at 6.9 and 8.3° are attributable to the ε and δ cocrystal components remaining in the specimen.